Liquid Crystals
Publication details, including instructions for authors and subscription information:
http://www.informaworld.com/smpp/title~content=t713926090

Crystal G phase induced through intermolecular hydrogen bonding IV: a study of crystallization kinetics

Pisupati Swathi; P. A. Kumar; V. G. K. M. Pisipati

Online publication date: 06 August 2010

To cite this Article Swathi, Pisupati , Kumar, P. A. and Pisipati, V. G. K. M.(2001) 'Crystal G phase induced through intermolecular hydrogen bonding IV: a study of crystallization kinetics', Liquid Crystals, 28: 8, 1163 — 1169
To link to this Article: DOI: 10.1080/02678290110038193
URL: http://dx.doi.org/10.1080/02678290110038193

LIQUID CRYSTALS, 2001, VOL. 28, NO. 8, 1163–1169

Crystal G phase induced through intermolecular hydrogen bonding IV†: a study of crystallization kinetics

PISUPATI SWATHI, P. A. KUMAR and V. G. K. M. PISIPATI*

Centre for Liquid Crystal Research and Education, Faculty of Physical Sciences, Nagarjuna University, Nagarjuna Nagar 522 510, India

(*Received 27 June 2000; in final form 28 November 2000; accepted 1 December 2000*)

A systematic crystallization kinetic study using thermal microscopy and differential scanning calorimetry has been carried out on two novel liquid crystalline compounds, DBA : MHB and DBA : ACP. These involve intermolecular hydrogen bonding between 4-*n*-decyloxybenzoic acid (DBA) and methyl 4-hydroxybenzoate (MHB); and between DBA and 2-amino-5-chloropyridine (ACP). The kinetics experiments were performed from the crystal G phase, which is a common induced kinetophase in both the compounds. Further, the proton donor and acceptor capabilities of the −COOH group of DBA towards the −OH group of MHB and −N= atom of ACP were studied in the light of mesomorphism and rate of crystallization. The dimensionality in the crystal growth and the sporadic nucleation were estimated from the Avrami exponent, *n*. A similar type of crystallization mechanism is predicted to operate for all the crystallization temperatures. The characteristic crystallization time (t^*) at each crystallization temperature is deduced from the individual plots of $\log t$ vs. ΔH (change in enthalpy).

1. Introduction

Since Kato and Frechet [1] reported a novel liquid crystal material induced by intermolecular hydrogen bonding between a pyridine nitrogen and a carboxylic acid, a number of liquid crystalline compounds involving hydrogen bonds have been synthesized; these include conventional liquid crystals (LCs) [2–8], and ferroelectric liquid crystals [9–11]. The formation of these hydrogen bonds plays a crucial role in self-assembling systems and the building of organized molecular structures [12]. The liquid crystallinity induced by the H-bond interactions shows a pronounced impact on mesogenic properties such as melting point, heat of vaporization and enthalpy of phase transition. Moreover, these non-covalent interactions with low bond and activation energies influence the rate of crystallization and the related nucleation mechanism.

It is well known [13, 14] that in conventional liquid crystals, crystallization kinetics of a particular mesophase arise when a stable lower temperature phase grows out of a mother metastable phase in the form of small domains, which are affected by temperature and time. During such a nucleation process the formation of an ordered domain occurs which converts to a stable nucleus that initiates the aggregation of the surrounding molecules to form layered domains. On the other hand, heat flow in these non-covalent self-organizing systems is rather a complicated process, and the nucleation and growth of domain across the molecular layers is solely dependent on the strength of hydrogen bonding with respect to temperature. In order to understand such a nucleation mechanism in these systems, the study of crystallization kinetics serves as a powerful tool and to the best of our knowledge no such attempt has been made in current research.

Recently, He *et al.* proposed [13] a theoretical model for the process of crystallization, involving sporadic nucleation and growth in two dimensions in columnar layers of a discotic liquid crystal. In continuation of our previous extensive crystallization kinetics investigations [14] in the smectic layers of well known *N*-(4-*n*-alkoxybenzylidene)-4-*n*-alkylanilines (commonly known as *n*O.*m* compounds), the present communication deals with the systematic crystallization kinetic study and the related nucleation process as for two novel liquid crystalline compounds, DBA : MHB and DBA : ACP. These compounds involve intermolecular hydrogen bonding between 4-*n*-decyloxybenzoic acid (DBA) and methyl 4-hydroxybenzoate (MHB); and between DBA and 2-amino-5-chloropyridine (ACP). In order to study the influence of proton acceptor (non-mesogenic) moieties on the rate of crystallization, 4-*n*-decyloxybenzoic acid was used as

*Author for correspondence;
e-mail: venkata_pisipati@hotmail.com
†For part III see [15].

Liquid Crystals ISSN 0267-8292 print/ISSN 1366-5855 online © 2001 Taylor & Francis Ltd
http://www.tandf.co.uk/journals
DOI: 10.1080/02678290110038193

a common mesogenic moiety in both compounds. The molecular structures of DBA : MHB and DBA : ACP are illustrated in figure 1.

2. Experimental

The synthesis and structural characterization of compounds, DBA : MHB and DBA : ACP are reported elsewhere [15]. By differential scanning calorimetry, using a Perkin-Elmer DSC-7 instrument, the crystallization rate was monitored by measuring the development of the crystal endotherm with time. Simultaneous phase identification at each crystallization temperature was carried out using a Mettler Toledo DSC (equipped with FP 99A central processor) supplemented by an Olympus polarizing microscope. The DSC scans were performed on each of the present compounds (3–5 mg) using aluminium and/or glass crucibles. The procedure for DSC scans at each crystallization temperature was reported earlier [14].

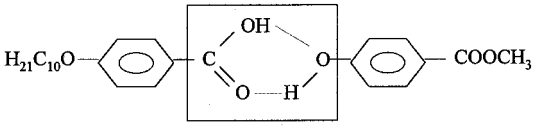

DBA:MHB

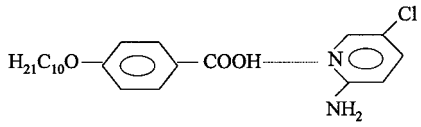

DBA:ACP

Figure 1. Molecular structures of DBA : MHB and DBA : ACP.

3. Results and discussion

By cooling the isotropic melt, the identification of phase variants in DBA : MHB and DBA : ACP was determined by their characteristic textures [16] using a polarizing thermal microscope. The transition temperatures of the phases observed through thermal microscopy were found to be in reasonable agreement with the corresponding DSC thermograms. The phase variants and the transition temperatures are summarized in table 1. DBA : MHB was found to exhibit characteristic texture: threaded marble texture in nematic, broken focal texture in C (SmC) and smooth mosaic texture in crystal G (G) phases. DBA : ACP showed a G phase as a smooth multi-coloured mosaic texture.

The method of thermal selectivity of crystallization temperatures was described in a previous communication [14]. The crystallization kinetics relating to the phase transition from crystal phase to melt for each compound was performed at each selected crystallization temperature (table 2).

Table 1. Transition temperatures (°C) from thermal microscopy and DSC of compounds DBA : MHB and DBA : ACP. Values on cooling in square brackets; enthalpies (J g^{-1}) in parentheses.

Compound	Phase variant	I–N/G	N–SmC	SmC–G	G–Cr
DBA : MHB	N/SmC/G	129 [127.3 (6.1)]	104 [104.1 92.9)]	94 [86.8 (35.1)]	76 [68.7 (25.1)]
DBA : ACP	G	72 [68.5 (11.8)]	—	—	54 [50.1 (82.6)]

Table 2. Measured crystallization parameters in the G phases of DBA : MHB and DBA : ACP.

Compound	Crystallization temperature/°C	Crystallization time (t^*)/min	x	n	b ($\times 10^{-1}$)
DBA : MHB	66	2.0	0.999	2.80	1.43
	67	4.0	0.998	1.38	1.47
	68	8.0	0.997	0.87	1.62
	70	16.0	0.997	0.65	1.64
	72	16.0	0.998	0.67	1.56
	74	32.0	0.998	0.53	1.59
	76	64.0	0.997	0.52	1.15
DBA : ACP	55	2.0	0.814	0.75	5.93
	56	4.0	0.860	0.49	5.06
	57	16.0	0.789	0.16	6.41
	58	32.0	0.868	0.20	4.93

3.1. *DBA : MHB*

The DSC thermograms of DBA : MHB are illustrated in figure 2. In the heating cycle, the compound exhibited three distinct transitions at 131.2 (N–I), 105.2 (SmC to N), 95.1 (G to SmC) and 87.7°C (C–G) with heats of transition 4.5, 1.9, 35.7 and 67.5 J g^{-1}, respectively. The cooling exotherm showed corresponding transitions at 127.3, 104.1, 86.8 and 68.7°C with their enthalpies, 6.1, 2.9, 35.1 and 25.0 J g^{-1}. These DSC thermograms clearly imply that the kinetics of crystallization from the G phase could be investigated over the temperature range 66 to 76°C.

Figures 3 and 4 illustrate typical DSC endotherm profiles for different time intervals at crystallization temperatures, 66 and 76°C, respectively. As shown in figure 3 the sample is held at 66°C for different time intervals. The heating curve recorded immediately at a

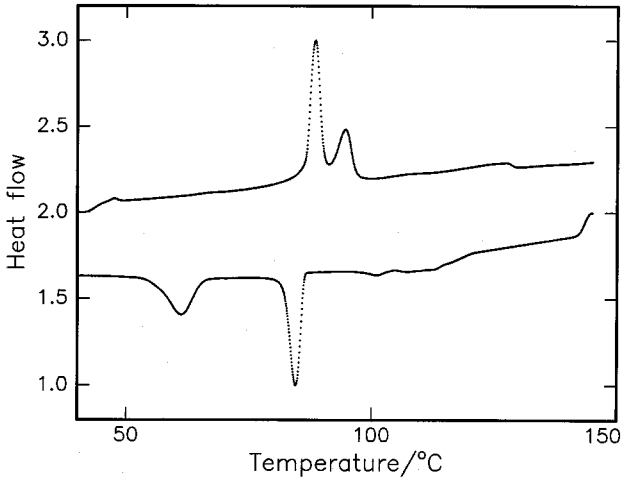

Figure 2. DSC heating and cooling thermograms of DBA : MHB.

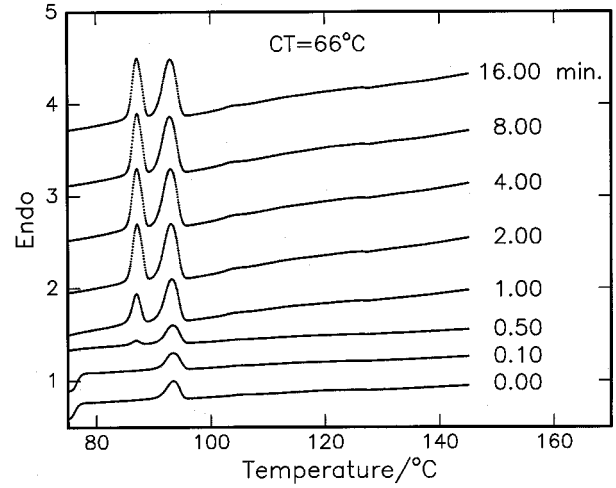

Figure 3. DSC endotherm profiles of DBA : MHB at 66°C for different time intervals.

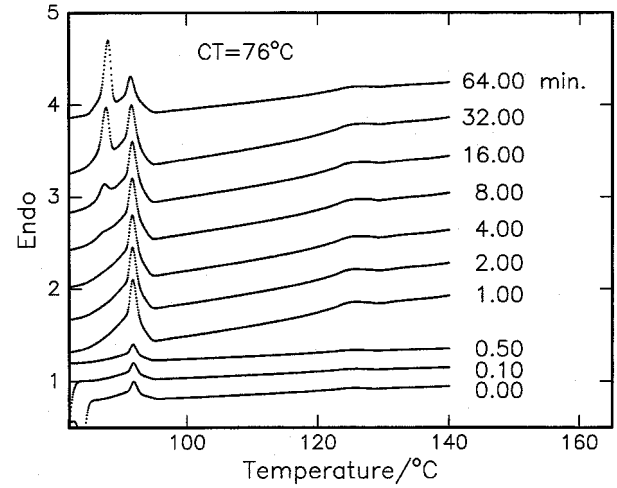

Figure 4. DSC endotherm profiles of DBA : MHB at 76°C for different time intervals.

crystallization time of $t = 0$ min following the quenching of crystal to melt, revealed the only G to SmC transition. However, the appearance of a small peak was observed after holding the sample for 0.50 min; this is attributed to a melting transition, suggesting a fast crystallization process. The extent of this melting transition increases with increase of time interval, and its growth continues until the time interval reaches 16 min. This process of crystallization can be attributed to the formation of a larger and larger crystal fraction with time, and this conversion process in the present case appears to be complete after 16 min. However, a glance at figure 4 showing endotherm profiles recorded at crystallization temperature 76°C for different time intervals, reveals an altogether different trend in the growth of the melting transition. As expected, the thermogram recorded at crystallization time $t = 0$ showed only a G transition. After holding the sample for 1 min, the melting transition appears to develop as a shoulder. This trend in the growth of the melting transition is critical in the sense that the crystallization process follows a unique mechanism over crystallization temperatures ranging from 66 to 70°C, which is seen from the corresponding endotherm profiles, where the melting transition starts as a distinct peak. However, in the temperature range 72 to 76°C the development of the melting peak shoulder (figure 4) clearly suggests a different nucleation mechanism. This trend may be attributed to the effective role and stability of hydrogen bonding; no further detailed attempt has been made at this stage to substantiate this selective anomalous thermal behaviour of the crystal growth mechanism.

3.2. *DBA : ACP*

Figure 5 shows DSC thermograms of DBA : ACP in heating and cooling cycles. The heating scan shows two

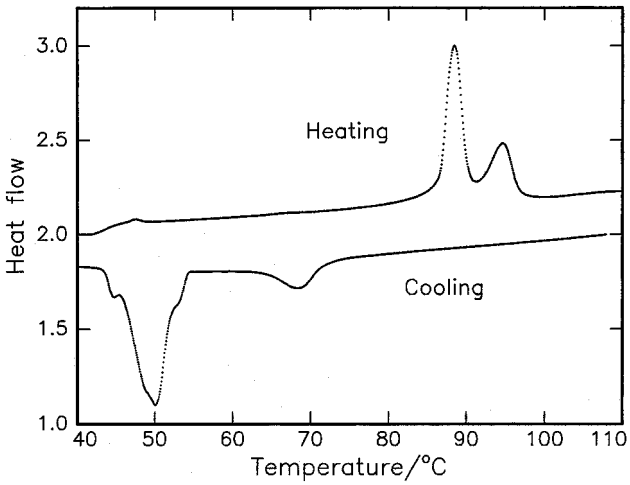

Figure 5. DSC heating and cooling thermograms of DBA : ACP.

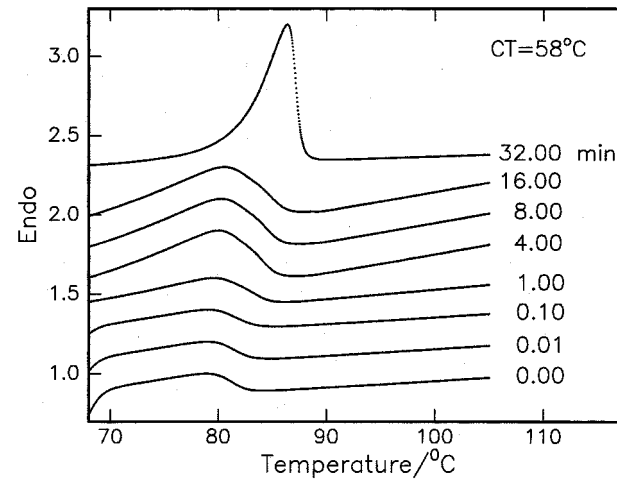

Figure 7. DSC endotherm profiles of DBA : ACP at 58°C for different time intervals.

significant transitions at 86.5 and 95.1°C, with the corresponding enthalpies 109.9 and 13.8 J g^{-1}, respectively. The former transition is assigned to a crystal to melting transition, the latter to a G to isotropic transition. On cooling the sample from its isotropic melt, the exotherm exhibits the transitions due to isotropic to G (68.5°C) and G to crystal (50.1°C); the corresponding enthalpy values are 11.8 and 82.0 J g^{-1}, respectively. The crystallization kinetics relating to the transitions from the G phase were selectively performed at the crystallization temperatures 54, 55, 56, 57 and 58°C. Typical DSC endotherm profiles for different time intervals at two crystallization temperatures, 55 and 58°C are presented in figures 6 and 7, respectively. The sample was held at 55°C for different time intervals (0.01 to 4.00 min). The heating curve recorded at crystallization time $t = 0$ min following the quenching of the crystal to melting transition at 55°C, displays only a G to isotropic transition, indicating the non-existence of a crystal to melting transition. However, at $t = 2$ min the sudden appearance of a crystal to melting transition suggests a fast crystallization process. It is useful to recall the trend in the growth of a similar transition in DBA : MHB, where the extent of this melting transition shows a gradual increase with time interval. The sudden increase of this transition can best be interpreted in terms of molecular contributions associated with the ACP moiety at the micro level. On the other hand, the endotherm profiles recorded at crystallization temperature 58°C for different time intervals (figure 7) show an altogether different trend for the crystallization kinetics. Interestingly, at $t = 0$, the DSC curve shows the formation of a melting transition with the non-existence of a crystal G transition. The growth of this transition continues and it finally emerges as a single predominant peak. The heat of transition of this peak is equal to the sum of individual enthalpies of the melting and crystal G transitions. This, however, clearly suggests that the process of crystallization at 58°C follows a delayed nucleation mechanism which has a pronounced impact on the temperature range of the liquid crystalline phase.

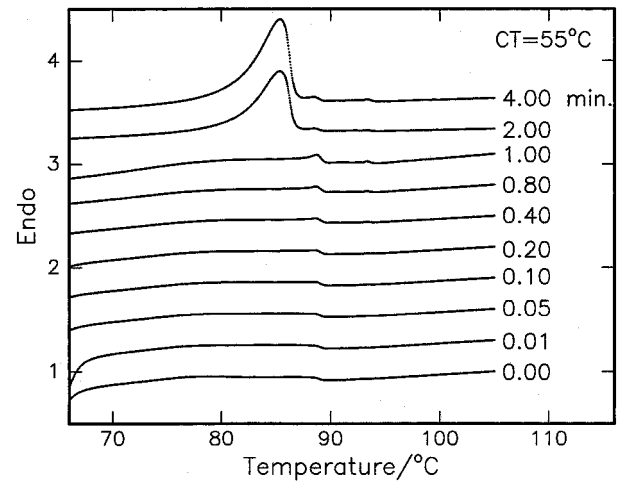

Figure 6. DSC endotherm profiles of DBA : ACP at 55°C for different time intervals.

3.3. *Crystallization kinetics*

The heats of transition for individual transitions at different time intervals have been calculated [14] for each crystallization temperature, and the data (table 2) plotted against the corresponding logarithm of time interval for each compound. Figures 8 and 9 show plots for DBA : MHB at 66 and 76°C and DBA : ACP at 55 and 58°C, respectively. The plots are identical in shape apart from the shift in the log t axis, suggesting the

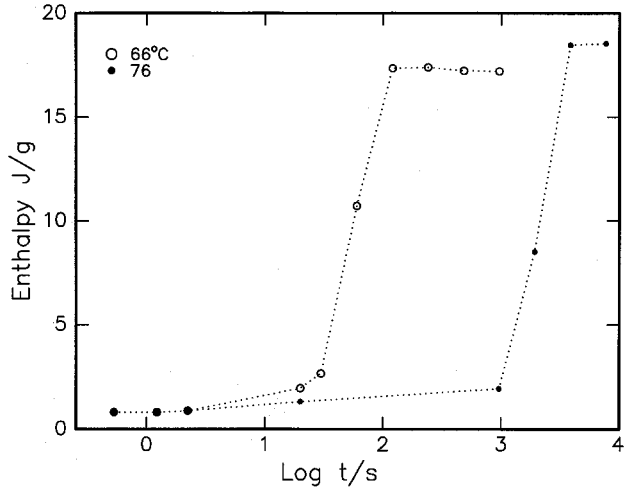

Figure 8. Heats of melting as a function of the logarithm of annealing time in the crystal G phase of DBA : MHB at 66 and 76°C.

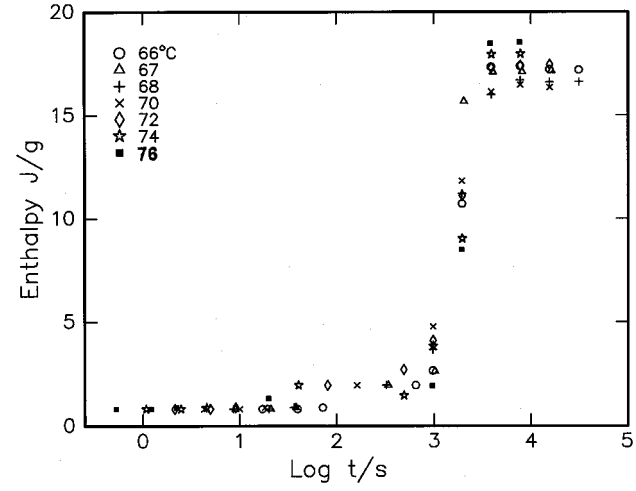

Figure 10. Master curve of enthalpies of the crystalline phase of DBA : MHB as a function of the logarithm of annealing time for different temperatures.

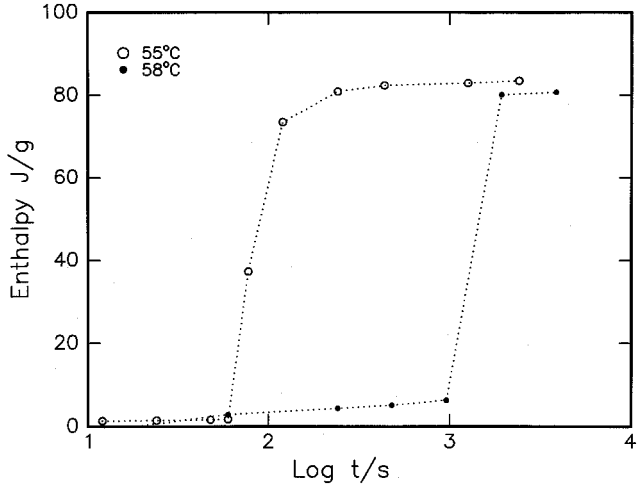

Figure 9. Heats of melting as a function of the logarithm of annealing time in the crystal G phase of DBA : ACP at 55 and 58°C.

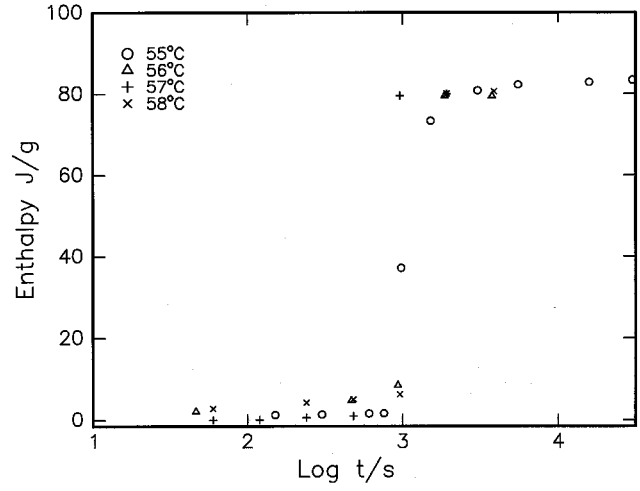

Figure 11. Master curve of enthalpies of the crystalline phase DBA : ACP as a function of the logarithm of annealing time for different temperatures.

limitations of rate of crystallization [13, 14]. Moreover, the simultaneous measurement of the enthalpy of the crystal G endotherm with time illustrates the effective beginning and end of the crystal formation process; this coincides with that of the formation of the melting transition. Further, plots of enthalpies of the mesogenic phase vs. the log of annealing time at different crystallization temperatures were obtained by shifting the data along the log t axis to 76°C (DBA : MHB) and 58°C (DBA : ACP), and are depicted in figures 10 and 11 respectively. The master curve for DBA : MHB (figure 10) clearly shows an increasing trend in the enthalpy values for higher crystallization temperatures (72 to 76°C); this provides substantial evidence for the existence of two different crystallization mechanisms operating over the entire crystallization thermal range. However, the overall crystallization rate in both compounds is controlled by nucleation rate and the rate of growth of domains [13].

4. Process of crystallization

The homogeneous process of nucleation involving the growth of small crystal domains leads to the phenomenon known as sporadic growth [13, 14]. As the temperature is lowered, the formation of an ordered domain occurs; this converts to a stable nucleus that initiates the aggregation of surrounding molecules to form layered domains. The origin of the nucleus is critical as its formation proceeds until it reaches a sufficient size to initiate the crystallization process. We propose that at this stage the crystallization process is controlled by

interlayer distances in the tilted G phase. This mode of conversion of lammellar layer correlation in the tilted phase is a rather complicated and slow process [14]. In such a process of seed nucleation, the factors associated with smectic layers play a crucial role. For example, a particular molecule in the lower smectic layer acquires a requisite energy to allow the formation of ordered domains, which in turn propagate crystallization in adjacent layers. These ordered domains will further proceed through the smectic layer by a process of successive addition of molecules from neighbouring layers, leading to sporadic nucleation and growth in two dimensions. This process continues until crystallization is complete. During this process, the contributions from crystal defects, impurities and solid state transformations affect the overall rate of phase transformation and the dimensional geometry of the growing domains. It is now well established that the crystallization process, involving the fraction of transformed volume x at a time interval t may be expressed in terms of the Avrami equation [17, 18]

$$x = 1 - \exp(-bt^n)$$

where the constants b and n depend on the nucleation mechanism and the dimensional geometry of the growing domains, respectively. At each crystallization temperature these constants were calculated as reported earlier [14]. It is found (table 2) that the constant n varies, with values ranging from 0.5 to 2.8 for DBA : MHB and from 0.1 to 0.7 for DBA : ACP. For $n = 3 \pm 0.1$, two possibilities exist for the crystallization process: a predetermined nucleation followed by a growth in three dimensions, or sporadic growth in two dimensions. The latter is more favourable for crystallization in smectic liquid crystals [13, 14]. However, for predictions on the growth dimensionality in the case of low n values, a detailed X-ray investigation is needed. The magnitude of the constant b, which governs the nucleation mechanism, is similar for both compounds, in the order of 10^{-1}. The trend in the magnitudes of these two constants is, however, inconsistent with data reported for other smectogens [14, 19]. On the other hand, in the case of DBA : MHB, the value of n at crystallization temperature 66°C is in reasonable agreement with data reported for a discotic mesogen [13].

5. Conclusions

The comparative kinetics studies performed on the tilted crystal G phases induced by H-bonding between *p-n*-decyloxybenzoic acid and two different non-mesogenic moieties, MHB and ACP, reveal different trends of crystallization behaviour between the two compounds. This suggests that the influence of the liquid crystalline moiety (DBA) on the crystallization behaviour is negligible. Unlike in the reported *n*O.*m* compounds [14], the value of the dimensionality parameter n varies at each crystallization temperature, and in most cases these values follow a decreasing trend with increasing temperature. Further, it is evident from the degree of variation in this parameter that at a particular crystallization temperature the compound exhibits an independent nucleation mechanism. A possible explanation for this anomalous crystallization behaviour may be the sporadic nucleation growth, which follows an inhomogeneous process of continuous nucleation over a constant time. We may add here that the hydrogen bond strength at a particular crystallization temperature has a dominating effect on the crystallization time. This can be understood on the basis of donor and acceptor tendencies of the pyridine nitrogen and hydroxyl groups towards the acid group of the DBA moiety. A detailed IR structural study on the reported DBA : MHB complexes [8] confirmed that −OH and −COOH groups are complementary to each other in forming the hydrogen bond by donating and accepting protons to one another. This, however, leads to the formation of a stable five-membered ring configuration; it is therefore reasonable to expect a high thermal energy to be required for the dissociation of this stable configuration. In contrast, the observed enthalpy values for DBA : MHB are found to be low in comparison with those of DBA : ACP. This result provides valuable information about the stability of the hydrogen bond at a given crystallization temperature. It is concluded that the strength of the hydrogen bond is greater when the pyridine nitrogen is involved. Moreover, at final crystallization temperatures DBA : MHB exhibits a slow rate of crystallization kinetics with a time interval of 64.0 min, while DBA : ACP shows a fast rate of crystallization with a time interval of 32 min.

The authors are thankful to the Department of Science and Technology, Council of Scientific and Industrial Research and University Grants Commission, New Delhi for financial support.

References

[1] Kato, T., and Frechet, J. M. J., 1989, *J. Am. chem. Soc.*, **111,** 8533.
[2] Barmatov, E. B., Pebalk, D. A., Barmatov, M. V., and Shibaev, V. P., 1997, *Liq. Cryst.*, **23,** 447.
[3] Tian, Y., Xu, X., Zhao, Y., Tang, X., and Li, T., 1997, *Liq. Cryst.*, **22,** 87.
[4] Letellier, P., Ewing, D. F., Goodby, J. W., Haley, J., Kelly, S. M., and Mackenzie, G., 1997, *Liq. Cryst.*, **22,** 609.
[5] Sideratou, Z., Tsiourvas, D., Paleos, C. M., and Skoulios, A., *Liq. Cryst.*, **22,** 51.

[6] Raju, S. V. N., Mule, S. A., Rajan, C. R., and Ponratnam, S., 1997, *Ind. J. Chem*., **36A** & **B,** 525.
[7] Kumar, P. A., Srinivasulu, M., and Pisipati, V. G. K. M., 1999, *Liq. Cryst*., **26,** 1339.
[8] Swathi, P., Kumar, P. A., and Pisipati, V. G. K. M., 2000, *Liq. Cryst*., **27,** 665.
[9] Yu, L. J., 1993, *Liq. Cryst*., **14,** 1303.
[10] Kumar, U., Kato, T., and Frechet, J. M. J., 1992, *J. Am. chem. Soc*., **114,** 6630.
[11] Kato, T., Kihara, H., Uryu, T., Ujie, S., Imura, K., Frechet, J. M. J., and Kumar, U., 1993, *Ferroelectrics*, **148,** 161.
[12] Paleo, C. M., and Tsiourvas, D., 1995, *Angew. Chem. int. Ed. Engl*., **34,** 1696.
[13] He, Z., Zhao, Y., and Caille, A., 1997, *Liq. Cryst*., **23,** 317.
[14] Kumar, P. A., Madhu Mohan, M. L. N., and Pisipati, V. G. K. M., 2000, *Liq. Cryst*., **27,** 727.
[15] Swathi, P., Sastry, S. S., Kumar, P. A., and Pisipati, V. G. K. M., 2000, *Mol. Cryst. liq. Cryst*. (to be published).
[16] Gray, G. W., and Goodby, J. W., 1984, *Smectic Liquid Crystals: Textures and Structures* (London: Leonard Hill).
[17] Avrami, M., 1939, *J. chem. Phys*., **7,** 1103.
[18] Avrami, M., 1940, *J. chem. Phys*., **8,** 212.
[19] Price, F. P., and Wendorff, J. H., 1971, *J. phys. Chem*., **75,** 2849; Price, F. P., and Wendorff, J. H., 1972, *J. phys. Chem*., **76,** 276.